JOURNAL OF MATERIALS SCIENCE 28 (1993) 955–962

Abrasive wear and craze breakdown in polystyrene

A. C.-M. YANG, T. W. WU
IBM Research Division, Almaden Research Center, 650 Harry Road, San Jose, CA 95120, USA

The role of craze breakdown during the fracture process of abrasive wear in glassy polystyrene was investigated. At first, the wear resistance, γ_w, was compared with the craze breakdown strain as a function of molecular weight and diluent concentration. It was found that γ_w increases with molecular weight and decreases with the diluent concentration. Although craze breakdown strain also increases with molecular weight and decreases with the diluent concentration, the wear data do not converge into a single curve in a plot against the craze breakdown strain. Selected specimens were then studied by micro-indentation and micro-scratching experiments. An analysis of the scratch patterns and contact load at the polymer surface indicated that a critical stress criterion, rather than a critical strain criterion, may be suitable for the onset of the failure process in brittle polymer wear. With this criterion, the critical load for crack opening, τ_c, can be related to the craze breakdown strain and Young's modulus, and the observed deviation between the craze breakdown strain and γ_w can be explained.

1. Introduction

The initial stage of abrasive wear in glassy polymers is the process of contact and scratch between the polymer surface and the sharp asperities. The microscopic failures occurring during scratch collectively generate loss particles and give rise to a weight loss. Undoubtedly, the illumination of the mechanism of the microscopic failures is critically important for understanding and controlling the complicated polymer wear. The failure mechanism may be the breakdown of the fine local deformation zones which normally precede crack propagation in glassy polymers. Yet, the role of the local deformation zone breakdown in abrasive wear of polymer glasses has never been studied carefully. In this paper, a model glassy polymer, polystyrene, was selected to study the relationship between the breakdown of crazes and the abrasive wear. The result should cast light on the general failure mechanisms of abrasive wear in the brittle polymer glasses.

Crazes [1–8] and shear deformation zones [9–14] are microscopic deformation zones in glassy polymers formed by mechanical stresses. Although both are precursors of crack propagation, they are quite different in terms of zone microstructure, mechanical strength, and molecular processes involved during the formation and breakdown. Crazes form when a hydrostatic tension exceeds the crazing stress, σ_c, at which the polymer is locally drawn into tiny fibrils to form the deformation zones. Once the fibrillation starts, crazes act as an "energy sink", absorbing the subsequently applied mechanical work, and eventually break down to trigger the brittle crack propagation. Shear deformation zones, on the other hand, are caused by the shear component of the applied stress and are formed in a more delocalized fashion than are crazes. Owing to the fact that the deformation zones can survive a much larger strain before breakdown, shear deformation is generally considered a ductile mode of failure, whereas crazing is a brittle mode. For abrasive wear, shear deformation is expected to dominate the early stage of abrasion before the critical dilatational stress for crazing is reached. Crazes, however, will eventually emerge as soon as the tension reaches σ_c and initiate crack propagation and material loss.

To measure the ductility of the crazes in different polymers, the ultimate strain corresponding to craze breakdown is statistically determined [1, 2] and has been used successfully in a number of glassy polymers [1, 2, 15]. The critical stress at which the craze fibrils fail, alternatively, is another way to characterize craze breakdown. To study the role of crazing during abrasive wear, the breakdown strain is used here first to compare with the measured wear resistance. The microscopic failure process during abrasion is further studied by the new techniques of micro-indentation and micro-scratching [17–20]. As will be shown later, the critical load for crack opening during scratching in fact is a useful parameter for predicting wear resistance. Furthermore, a critical stress criterion can be established for the weight loss process during polymer abrasion.

2. Experimental procedures

Two series of polystyrenes (PS) were prepared for tests: (1) monodisperse PS with molecular weight (MW) of 13×10^3, 47.3×10^3, 90×10^3, 400×10^3,

0022–2461

900×10^3, 2×10^6 and 20×10^6, and (2) blends of high MW PS (MW = 2×10^6) and low MW PS oligomers (MW = 2×10^3) with the volume fraction, χ (of the high MW species) ranging from 0.1–1.0. The polymer was cast from a toluene solution on to a substrate and dried under ambient conditions followed by heating in a vacuum at 120 °C for 48 h to remove the residual solvents. The thickness of the cast polymer layer is approximately 100 μm for abrasion samples and 20 μm for micro-indentation and micro-scratched samples. In both cases, the samples were thick enough to avoid the substrate effect. During sample preparation, fine cracks were noticed to form in the extremely brittle samples, e.g. the MW = 13×10^3 PS and $\chi = 0.1$ blend. These specimens, however, were still used because they were otherwise intact and the fine cracks showed no detectable effects (e.g. to start large-scale cracking or delamination) on the subsequent abrasion tests.

The abrasion test was conducted in a Taber abrader (Taber Instruments Corporation; e.g. ASTM C501) as shown in Fig. 1a. The sample was clamped to a rotating stage (constant speed at ~60 r.p.m.) on which it was abraded by a pair of Al_2O_3-containing abrasive wheels (standard CS-10 calibrases). Each of the abrasive wheels was under a load of 400 g. During the test, the wear debris was constantly removed by two vacuum nozzles and, for every 200 cycles, the weight loss was measured while the abrasive wheels were refaced. Before each weight measurement, the worn surface was cleaned with a gentle air flow.

Micro-indentation and micro-scratching tests were carried out using an instrument constructed by Wu *et al.* [17–19], which is shown in Fig. 1b. For an indentation test, a three-sided pyramidal diamond indentor was used. The normal load at the tip and the penetration depth were recorded simultaneously, which can be used for hardness calculation, and the Young's modulus was determined from the slope of the unloading curves [20]. In a micro-scratching test, the indentor used was a conical diamond tip with a nominal 5 μm radius. The tip moved at a fixed velocity (of 1 μm s^{-1} in sliding and 15 nm s^{-1} in indentation) into the polymer. The normal load, τ, was measured during scratching which spans a distance of 150 μm. The scratch tracks on the polymer surface were subsequently examined by scanning electron microscopy. To eliminate the problem of spot-to-spot variation, usually six scratches or so were made in one sample to ensure data reproducibility. The resolutions of the applied load and penetration depth are about 30 μN and 1 nm, respectively.

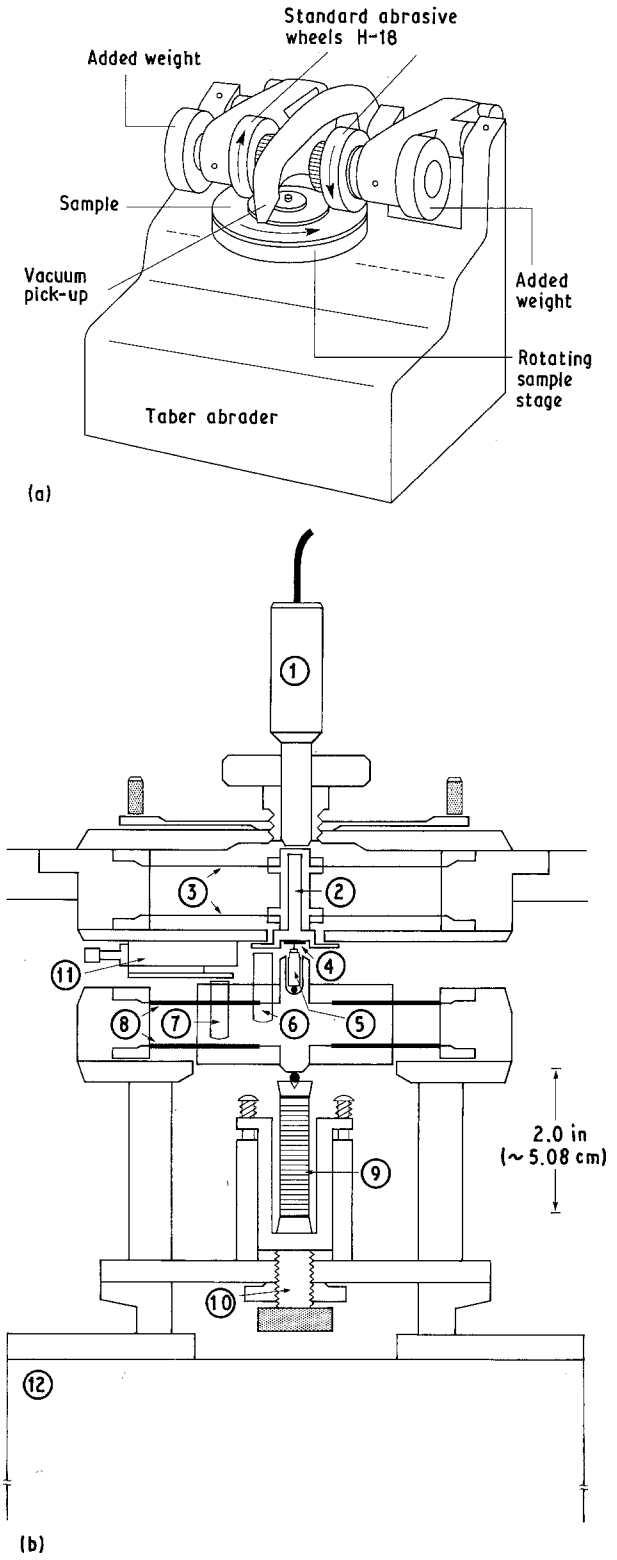

Figure 1 Schematic drawing of (a) the Taber Abrader, and (b) the micro-indentation/micro-scratching apparatus. 1, Load cell capacitance probe; 2, sample post; 3, 8, Be–Cu diaphragm springs; 4, sample; 5, indentor; 6, sample capacitance probe; 7, indentor capacitance probe; 9, PZT stack; 10, PZT pre-load mechanism; 11, reference plane stage; 12, Z-stage.

3. Results

3.1. Abrasive wear resistance

For all specimens, both the monodisperse PS and the PS blends, the weight loss was found to increase linearly with abrasion cycles, indicative of a steady-state wear prevailing during the test. The wear rate, R_w, weight loss per cycle, can be easily measured and the reciprocal of R_w is taken as the wear resistance, $\gamma_w \equiv 1/R_w$. Fig. 2 shows the wear resistance, γ_w, for both the monodisperse PS and the PS blends. As the molecular weight increases, wear resistance, γ_w, increases rapidly for the MW range 13×10^3–90×10^3, then levels off for MW > 200×10^3. For PS blends, γ_w increases approximately linearly with increasing volume fraction, χ, of the high MW PS. This behaviour of wear resistance, γ_w, was subsequently compared to the craze breakdown strain.

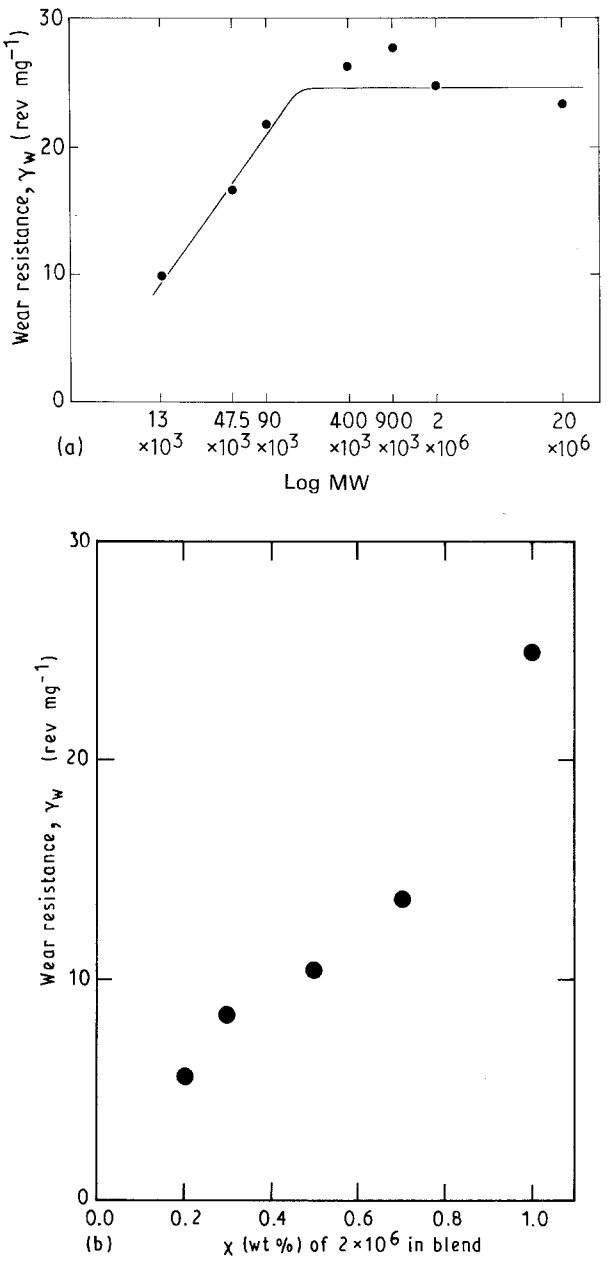

Figure 2 The wear resistance, γ_w, of (a) the monodisperse MW PS, and (b) the PS blends.

3.2. Comparison with craze breakdown strain

Craze breakdown strain was measured previously [1, 2] using statistical optical microscopy. In that experiment, a thin PS film was cast from solution and bonded on to a supporting copper grid [7] which effectively subdivided the film into a number of film squares defined by the copper meshes. The sample was then stretched uni-axially during which the film square was intermittently examined under an optical microscope to count the number fraction of film squares that underwent craze initiation or local craze breakdown. The difference between the median strains corresponding to craze initiation and breakdown was referred to as "craze fibril stability", and is used here as the breakdown strain of crazes. The median strain for craze initiation is usually small and can be neglected. It was measured to be approximately 0.8% independent of molecular weight and χ for the specimens tested here [1, 2].

Craze breakdown strain, ε_b, is shown in Fig. 3 for both the monodisperse PS and PS blends. It is interesting to note that, ε_b was found to behave very similarly to the wear resistance, γ_w, of both systems. Following the trend of wear resistance γ_w, ε_b increases rapidly as the molecular weight increases from 37×10^3 to 200×10^3 and levels off thereafter. It also increases linearly with increasing χ, the high MW PS concentration. These results demonstrate a clear trend that a higher ε_b leads to a higher wear resistance, γ_w. It also indicates that the mechanical failure that causes abrasive weight loss is controlled by a cracking process initiated by craze breakdown.

However, it was found that when the wear rate, R_w, of the two PS systems (monodisperse PS and PS blends) was plotted together versus ε_b, the data did not converge into a single curve, as shown in Fig. 4. This seems to indicate that the breakdown strain, ε_b, is not the only parameter dictating wear resistance. In addition, a subtle deviation between the curves of γ_w and ε_b was noticed. For the very fragile specimens where the craze breakdown strain $\varepsilon_b \simeq 0$, the wear resistance, γ_w, still shows a finite, although small, value. This behaviour probably can be attributed to the combination of the effect of plastic yielding and the limitation of wear testing, which will be discussed further below. The microscopic failure process during

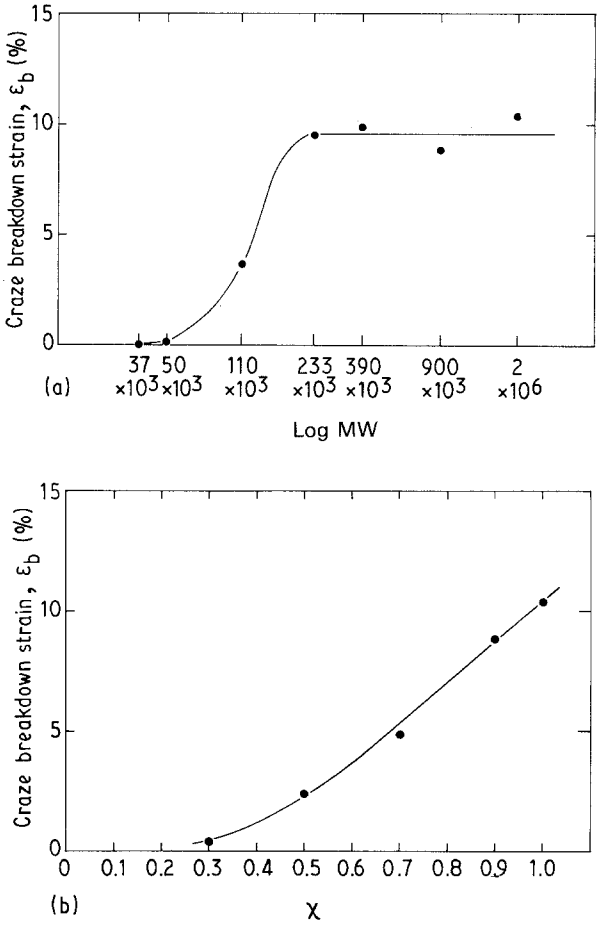

Figure 3 Craze breakdown strain, ε_b, of (a) monodisperse MW PS, and (b) the PS blends, [1, 2].

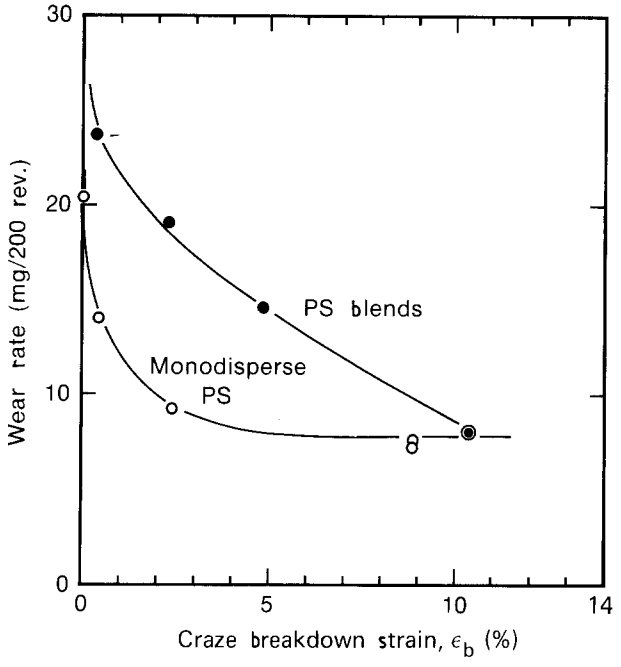

Figure 4 Wear rate versus the craze breakdown strain, ε_b, in PS.

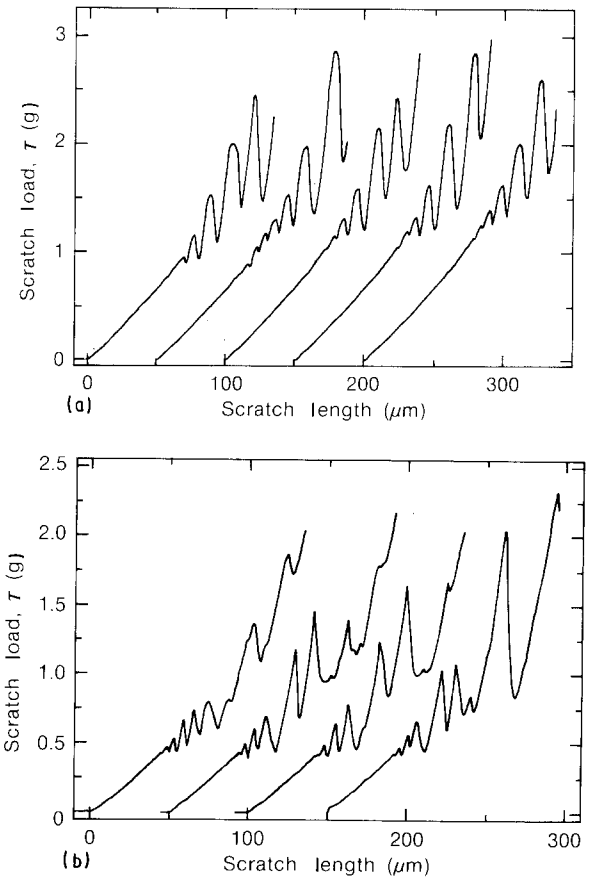

Figure 5 Contact load, τ, versus scratch distance of (a) MW = 90×10^3 PS, and (b) $\chi = 0.5$ blend.

polymer abrasion was further studied by using the new techniques of micro-indentation and micro-scratching. Two PSs, MW = 90×10^3 PS and $\chi = 0.5$ blend, were selected for these experiments because they have a comparable craze breakdown strain, ε_b, but quite different wear resistance, γ_w.

3.3. Critical load and scratch pattern

Fig. 5 shows the normal load, τ, measured at the conical diamond tip when the tip scratches into the PS. Clearly, the normal load, τ, increases linearly with the scratch distance in the beginning but when it reaches a threshold τ_c, it drops rapidly and undergoes large fluctuation. As revealed by the scanning electron micrographs of the scratch patterns (Fig. 6), the initial linear increase of load, τ, is evidently caused by the increase of the yielded volume, and the rate of load increase should be related to the hardness of the material scratched. The large load fluctuations, on the other hand, were clearly due to the consecutive cracking which caused a series of load releasing and load rebuilding events. The interesting semi-regular pattern of the cracks within the scratch track was initiated by the maximum tangential stress lying at the rear end of the travelling stylus ($x = -a$, $y = 0$). Schematically depicted in Fig. 7 is the proposed cracking process, in which Steps 3 and 7 represent the crack initiation by the dilatational stress behind the tip. The critical load, τ_c, therefore can be related to the craze breakdown strain, ε_b.

Although the two PS have similar curves of scratch load, τ, and similar scratch patterns, the critical load, τ_c, for crack opening is about twice as high for MW = 90×10^3 PS than that for $\chi = 0.5$ blend (1.0 g versus 0.45 g). Therefore, given the same loading conditions in a macroscopic abrasion where, in fact, a broad distribution of asperity load is characteristic of the contact between the polymer surface and the abrasive counterpart, the $\chi = 0.5$ blend is expected to undergo cracking much faster than the MW = 90×10^3 PS, thus demonstrating a lower wear resistance. This is consistent with the wear experiment results, and also implies that a load criterion is probably more suitable than a critical strain criterion for the brittle polymer wear.

3.4. Stress analysis and hardness measurements

The mechanical relationship between the contact load and the craze breakdown strain at the onset of cracking was examined by assuming linear elasticity for the abrasive contact. This assumption is reasonable due to the brittleness of the PS tested. At the stress concentration ($x = -a, y = 0$), the tensile stress in the x-axis, σ_{xx}^{tot} (Fig. 7) is the sum of the tangential and normal components, i.e.

$$\sigma_{xx}^{tot} = \sigma_{xx}^{T} + \sigma_{xx}^{N} \quad (1)$$

which, by assuming a Hertzian sliding contact, can be expressed as [21]

$$\sigma_{xx}^{T} = \frac{3(4 + \nu)}{16}\frac{\mu_f \tau}{a^2} = \frac{3\pi}{32}(4 + \nu)\mu_f \sigma_0 \quad (2)$$

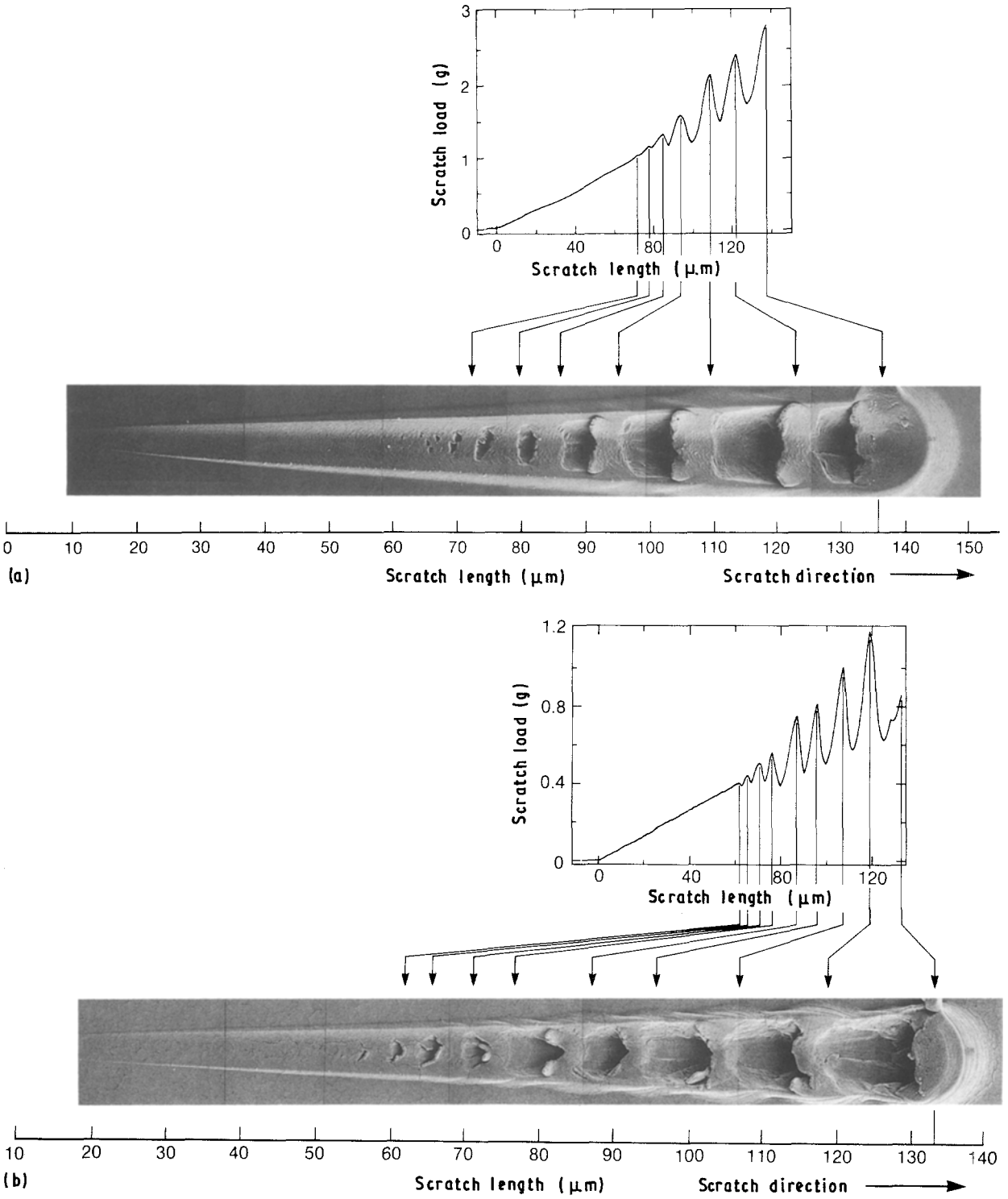

Figure 6 Scratch patterns of (a) MW = 90×10^3 PS, and (b) $\chi = 0.5$ blend, produced in the micro-scratching tests.

$$\sigma_{xx}^{N} = \frac{(1 - 2\nu)}{2\pi}\frac{\tau}{a^2} = \frac{(1 - 2\nu)}{4}\sigma_0 \quad (3)$$

where the stress $\sigma_0 = 2\tau/\pi a^2$, μ_f is the friction coefficient, and ν Poisson's ratio. Therefore, the total stress in the x-axis is

$$\sigma_{xx}^{tot} = \sigma_{xx}^{T} + \sigma_{xx}^{N} = \sigma_0(\alpha\mu_f + \beta) \quad (4)$$

where α and β are material constants, $\alpha = (3\pi/32)(4 + \nu)$ and $\beta = (1 - 2\nu)/4$. At the onset of cracking, the critical stress, $\sigma_{c,xx}^{tot}$, should be equal to the breakdown stress of craze fibrils, i.e.

$$\sigma_{c,xx}^{tot} = \sigma_{0,c}(\alpha\mu_f + \beta) \simeq E\varepsilon_b \quad (5)$$

The friction coefficient, μ_f, can be treated as a material constant for PS, as indicated by the measurements by both the conventional methods [22, 23] and the

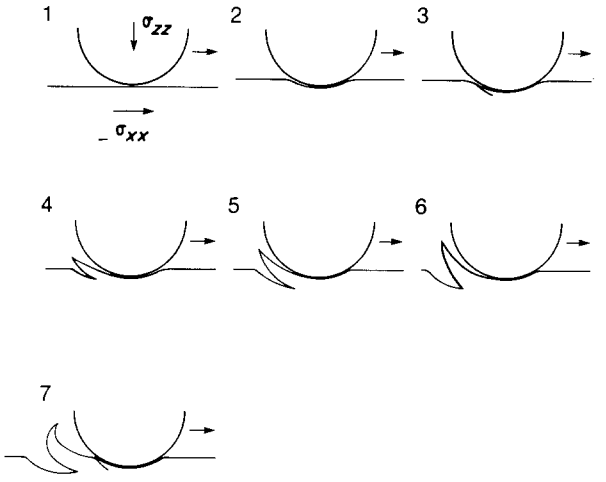

Figure 7 Schematic depiction of scratch deformation and cracking in a polymer by a conical stylus.

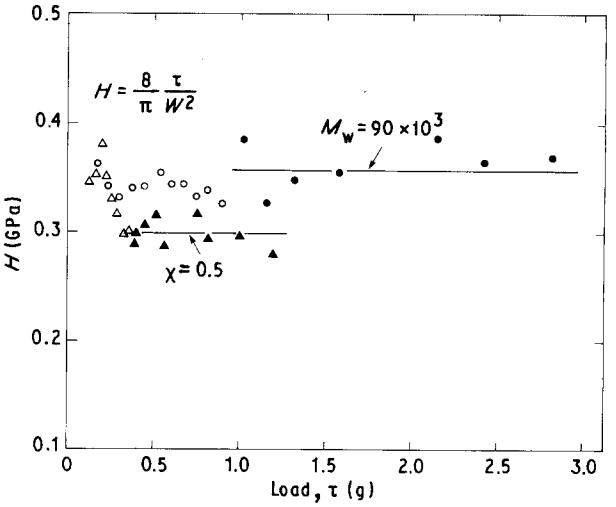

Figure 8 Scratch hardness versus the contact load determined from the micro-scratching tests. MW = 90×10^3 PS: (○) Before cracking and (●) after cracking. $\chi = 0.5$ blend: (△) before cracking and (▲) after cracking.

micro-scratching technique [24]. Hence, we have

$$\sigma_{0,c} = \frac{2}{\pi a^2}\tau_c \propto E\varepsilon_b \quad (6)$$

Equation 6 can be regarded as the failure criterion (critical stress) for abrasive wear in the brittle polymer glasses.

To test whether Equation 6 is indeed followed by the PS, the material data of the MW = 90×10^3 PS and $\chi = 0.5$ blend were substituted into the equation. Because the craze breakdown strains, ε_b, are approximately the same, the ratio of the stresses, $\sigma_{0,c}$, of the two materials (MW = 90×10^3 PS and $\chi = 0.5$ blend) should be approximately equal to the ratio of the Young's moduli. The stress $\sigma_0 = 2\tau/\pi a_2$, in fact, is the scratch hardness, defined as $H = \tau/A$, and can be measured along the scratch track by using τ and the projected contact area, A, from $A = \pi a^2/2$, where a is the radius of the projected contact area.

Fig. 8 shows the data of the scratch hardness as a function of load, τ, for the samples of MW = 90×10^3 PS and $\chi = 0.5$ blend. Apparently the two materials behave quite differently. For MW = 90×10^3 PS, the scratch hardness, H, is equal to 0.35 GPa, independent of the scratch length. For $\chi = 0.5$ blend, H starts at about 0.35 GPa at low τ but decreases continuously to 0.30 GPa at the onset of the first crack initiation, after which it remains constant. The explanation for the decrease in H before the first cracking in $\chi = 0.5$ blend is unclear. However, the levelled off value at the large scratch distance, 0.30 GPa, was taken as the scratch hardness of the blend because it is the measurement at the threshold of cracking. For the purpose of independent verification, the indentation hardnesses of these two samples were also measured by the micro-indentation method [17–19]. The results are shown in Fig. 9, for the indentation loading curves, and in Fig. 10, the indentation hardness depth profiles. The indentation hardness was determined from the asymptotic value of hardness at large penetration depths. Clearly, the values of the indentation hardness

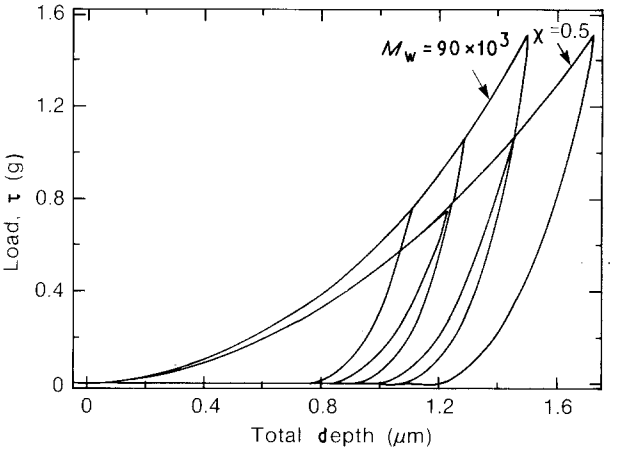

Figure 9 Indentation loading/unloading curves of MW = 90×10^3 PS and $\chi = 0.5$ blend in a micro-indentation test.

are very close to that of the scratch hardness for both the MW = 90×10^3 PS and the $\chi = 0.5$ blend.

The Young's modulus, E, was obtained from the indentation test by using the initial slope of the unloading curve in the indentation loading curves, shown in Fig. 9, where the elastic behaviour dominates [20]. The Young's modulus, E, was found to be 5.2 GPa for the MW = 90×10^3 PS, and 4.5 GPa for the $\chi = 0.5$ blend.

From these measurements, the ratio of the hardness (or the stress) $\sigma_{0,c}$(MW = 90×10^3 PS)/$\sigma_{0,c}$($\chi = 0.5$ blend), was determined to range from 1.15–1.22. The ratio of Young's moduli, E(MW = 90×10^3 PS)/E($\chi = 0.5$ blend) was measured to be around 1.16. The results are in good agreement with Equation 6. It demonstrates that craze breakdown is indeed the failure mechanism responsible for cracking and for the weight loss during abrasion in PS. A critical load criterion combining the craze breakdown strain, ε_b, and Young's modulus, E, appears to be suitable to describe the onset of this cracking process in the wear of brittle polymers.

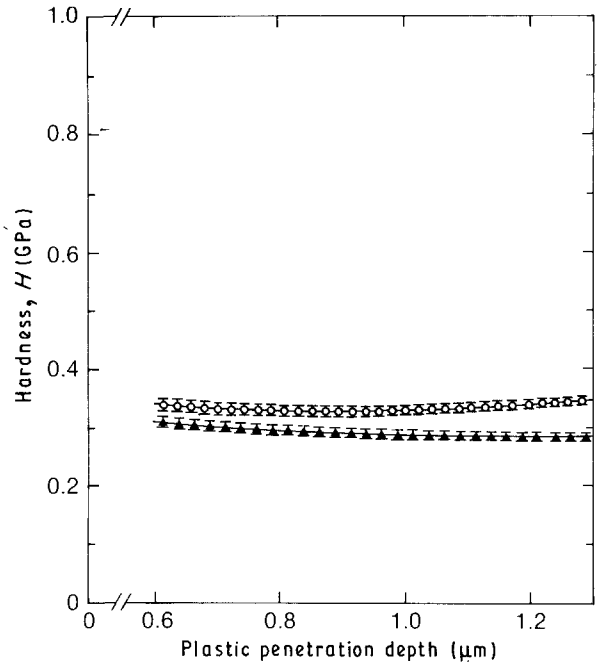

Figure 10 Indentation hardness of (○) MW = 90×10^3 PS and (▲) $\chi = 0.5$ blend measured from the micro-indentation tests.

4. Discussion

The fact that the extremely weak PS which have almost zero craze breakdown strain, ε_b, still demonstrate a small but finite wear resistance probably is due to the combination of yielding effect and the limitations of testing conditions. The yielding prior to cracking, as shown in the scratch patterns in Fig. 6, can provide an energy dissipation mechanism particularly for the PS with a low glass transition temperature, T_g. In these materials, the abraded regions may yield substantially before cracking, absorbing proportionally more mechanical work, and in effect show higher wear resistance. This plastic yielding effect, however, is still secondary compared to the effect of craze breakdown during the abrasion. As indicated clearly by the general trend of wear resistance in both the monodisperse PS and the PS blends, craze breakdown evidently dominates the failure processes of abrasive wear. On the other hand, due to the testing conditions of wear, there exists an upper bound on the amount of abraded material to be generated and removed. This limit translates into a lower bound of the wear resistance, γ_w, measurable for the very brittle polymers.

The results obtained here for PS may apply to other polymer glasses where crazing precedes crack propagation. With this connection, the abrasive wear behaviour of polymer glasses can be understood from, and manipulated by, our knowledge of craze formation and breakdown. On the other hand, when the microdeformation mechanism switches, e.g. from crazing to shear yielding, the wear behaviour is expected to change substantially. It had been claimed that the abrasive wear rate of polymers falls on to a universal linear line when plotted against the parameter of so-called "cohesive energy" [25]. The "cohesive energy" was calculated from additive constants from the data of solubility and latent heat of each constituent atom or atom group within the molecule. Although this result demonstrates the important effect of the breakdown of polymer molecules on wear, it may, however, have oversimplified the wear mechanisms for individual polymers because polymers fail by different molecular mechanisms and the wear debris, in general, is much larger than the atomic scale. A recent study of the miscible polymer blend, PS and poly(2,6-dimethyl-1,4-phenylene oxide) (PPO), indicates that the wear rate versus blend composition actually shows a dependence composed of two linear lines that join at a composition close to the crazing–shear yielding transition [24]. This indicates that the identification of failure mechanisms is a key to understand the complicated wear process in polymers and the approach taken here can be extended to the ductile polymers that also fail by shear yielding.

5. Conclusions

1. Craze breakdown is the major failure mechanism in abrasive wear of PS and probably other brittle polymer glasses that under comparable conditions craze before crack propagation.

2. The wear resistance of PS increases rapidly with molecular weight from MW = 13×10^3–90×10^3, then levels off when the molecular weight increases continuously. However, it decreases linearly with concentration of the low MW diluents.

3. In PS wear resistance, γ_w, generally increases with the breakdown strain of crazes but the craze breakdown strain has been shown to be not the only parameter dictating wear resistance. Rather, a critical stress criterion appears to be suitable for the failure process that leads to abrasive weight loss in this class of polymer. In this criterion, the critical load for crack opening can be related to the craze breakdown strain and Young's modulus. The critical load for crack opening during scratching, τ_c, is an important material parameter for predicting the polymer wear resistance.

References

1. A. C.-M. YANG, E. J. KRAMER, C. C. KUO and S. L. PHOENIX, *Macromolecules* **19** (1986) 2010.
2. *Idem, ibid.* **19** (1986) 2020.
3. S. RABINOWITZ and P. BEARDMORE, *CRC Rev. Macromol. Sci.* **1** (1972) 1.
4. R. P. KAMBOUR, *J. Polym. Sci. D* **7** (1973) 1.
5. A. N. GENT, *AMD (Symp. Ser.) (Amer. Soc. Mech. Eng.)* **19** (1976) 55.
6. E. J. KRAMER, *Adv. Polym. Sci.* **52/53** (1983) 1.
7. B. D. LAUTERWASSER and E. J. KRAMER, *Philos. Mag.* **A39** (1979) 469.
8. A. N. GENT and A. G. THOMAS, *J. Polym. Sci. A2* **10** (1972) 571.
9. W. WHITNEY, *J. Appl. Phys.* **34** (1965) 3653.
10. D. H. ENDER and R. D. ANDREWS, *ibid.* **36** (1965) 3057.
11. A. S. ARGON, R. D. ANDREWS, J. A. GODRICK and W. WHITNEY, *ibid.* **39** (1968) 1899.
12. E. J. KRAMER, *J. Macromol. Sci. Phys.* **B10** (1974) 191.
13. J. C. M. LI and J. B. C. WU, *J. Mater. Sci.* **11** (1976) 445.
14. J. B. C. WU and J. C. M. LI, *ibid.* **11** (1976) 434.
15. L. L. BERGER, *Macromolecules* **23** (1990) 2926.
16. A. C.-M. YANG and E. J. KRAMER, *J. Polym. Sci. Polym. Phys. Ed.* **23** (1985) 1353.

17. T. W. WU, C. HWANG, J. LO and P. S. ALEXOPOULOS, *Thin Solid Films* **166** (1988) 299.
18. T. W. WU, R. A. BURN, M. M. CHEN and P. S. ALEXOPOULOS, *Mater. Res. Soc. Symp. Proc.* **130** (1989) 117.
19. T. W. WU, *J. Mater. Res.* **6** (1991) 407.
20. M. F. DOERNER and W. D. NIX, *J. Mater. Res.* **1** (1986) 601.
21. G. M. HAMILTON and L. E. GOODMAN, *J. Appl. Mech.* **33** (1966) 371.
22. H. POTENTE and R. KRUGER, *Farbe und Lack* **84** (1978) 72.
23. E. HORNBOGEN and K. SCHAFER, in "Fundamentals of Friction and Wear of Materials", edited by D. A. Rigney (ASM, Metals Park, OH, 1981) p. 409.
24. A. C.-M. YANG and T. W. WU, *Bull. Amer. Phys. Soc.* **36** (1991) 685.
25. J. P. GILTROW, *Wear* **15** (1970) 71.

Received 16 September 1991
and accepted 25 June 1992